

## ARTICLE

## Evaluation of Stress and Hydrogen Concentration at Grain Boundary of Steels Using Three-Dimensional Polycrystalline Model

Ken-ichi EBIHARA\*, Mitsuhiro ITAKURA, Masatake YAMAGUCHI,  
Hideo KABURAKI and Tomoaki SUZUDO

*Japan Atomic Research Agency, 2-4 Shirakata, Tokai-mura, Ibaraki-ken, 319-1195, Japan*

The decohesion model in which hydrogen segregating at grain boundaries reduces cohesive energy is considered to explain hydrogen embrittlement. Although there are several experimental and theoretical supports of this model, its total process is still unclear. In order to understand hydrogen embrittlement in terms of the decohesion model, therefore, it is necessary to evaluate stress and hydrogen concentration at grain boundaries under experimental conditions and to verify the grain boundary decohesion process. Under this consideration, we calculated the stress and the hydrogen concentration at grain boundaries in the three-dimensional polycrystalline model which was generated by the random Voronoi tessellation. The crystallographic anisotropy was given to each grain as a characteristic. As the boundary conditions of the calculations, data extracted from the results calculated in the notched round-bar specimen model under the tensile test condition in which fracture of the steel specimen is observed was given to the polycrystalline model. As a result, it was found that the evaluated stress does not reach the fracture stress estimated under the condition of the evaluated hydrogen concentration by first-principles calculations. Therefore, it was considered that the initiation of grain boundary fracture needs some factors except the stress concentration due to the crystallographic anisotropy.

**KEYWORDS:** *hydrogen embrittlement, grain boundary, polycrystalline model, tensile test, notched round-bar specimen, finite element method, finite volume method, first-principles calculation*

### I. Introduction

Hydrogen embrittlement is one cause of cracking in steels which is observed as delayed fracture of high strength steels and cold cracking at the heat affected zone of welds. Among several models that can explain hydrogen embrittlement,<sup>1-5)</sup> the decohesion model<sup>3,4)</sup> is one of plausible candidates. In this model, the embrittlement results from the reduction of cohesive energy at grain boundaries due to hydrogen segregation. In the tensile test of high strength steels, the intergranular fracture mode is observed in specimens charged hydrogen, and it is reported that the stress and the hydrogen concentration in the vicinity of the crack initiation dominate the fracture process.<sup>6)</sup> According to the first-principles calculation, it is confirmed that hydrogen is one of the elements which can reduce the cohesive energy of grain boundaries and the cohesive energy reduction by hydrogen is almost similar to phosphorous.<sup>7)</sup> Although these supports of the decohesion model for hydrogen embrittlement are reported, its total process is still unclear. In order to fully understand the mechanism of hydrogen grain boundary embrittlement in terms of the decohesion model, it is necessary to evaluate stress and hydrogen concentration at grain boundaries under experimental conditions and to verify the decohesion process of the grain boundary. In addition, the quantitative comparison with experiments is necessary.

According to the recent development of the experimental method and the numerical analysis method for thermal de-

sorption spectrometry (TDS),<sup>8-9)</sup> it is possible to evaluate the hydrogen concentration at grain boundaries in steels experimentally. However, it is difficult in the realistic condition that the specimen is thick and strained because the influence of the hydrogen diffusion and the stress inside the specimen on the TDS measurement becomes remarkable. The experimental evaluation of the stress at grain boundaries is also difficult. Therefore the numerical evaluation of the stress and the hydrogen concentration at grain boundaries is necessary.

In order to evaluate the stress and the hydrogen concentration at grain boundaries under the tensile test condition, in this paper, we calculated the stress and the hydrogen concentration in the model of the notched round-bar specimen under the tensile test condition reported previously<sup>6)</sup> first. Next we extracted the distributions of the displacement and of the hydrogen concentration around the stress concentration region, which was near the notch root, and used the extracted data as the boundary condition of the calculation in the polycrystalline model, which was generated by the random Voronoi tessellation as reported in the paper.<sup>10)</sup> The Voronoi cell and the interface between the Voronoi cells were regarded as the grain and the grain boundary of the polycrystalline model, respectively, and the crystallographic orientation was given to each grain (cell) randomly as a characteristic. From the calculation result of the polycrystalline model, we evaluated the stress and the hydrogen concentration at the grain boundaries of the notched round-bar specimen under the tensile test condition. The data flow of the calculations is summarized in **Fig. 1**. Furthermore, in

\*Corresponding author, E-mail: ebihara.kenichi@jaea.go.jp

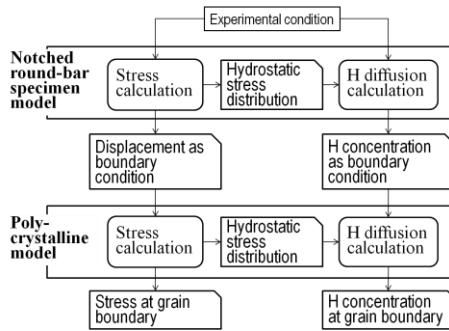


**Fig. 1** Data flow of the evaluation of the stress and the hydrogen concentration at grain boundaries of the polycrystalline model

order to examine the possibility of the grain boundary decohesion by the stress concentration due to the crystallographic anisotropy, we compared the evaluated stress with the fracture stress which was estimated under the condition of the evaluated hydrogen concentration by first-principles calculations.

This paper is organized as follows. The next section describes the calculation conditions of the notched round-bar specimen model and the polycrystalline model. The calculation results of both models are described in the third section. In the fourth section, we discuss the calculation results and the possibility of the grain boundary decohesion. The paper is summarized in the final section.

## II Calculation Conditions

### 1. Calculation Methods

We used the finite element method (FEM) for the stress calculation and the finite volume method (FVM) for the hydrogen diffusion calculation. Our FEM code is the improved one of the Adventure\_Solid code developed under the ADVENTURE project,<sup>11)</sup> and has two additional functions; one is the option of nonlinear hardening law, and the other is a capability of analyzing orthotropic materials. The FVM code is our developing code which solves numerically the following equation,<sup>4,12)</sup>

$$\frac{\partial C}{\partial t} = D_H \nabla^2 C - \frac{D_H V_H \nabla(C \nabla \sigma_h)}{RT}. \quad (1)$$

This equation describes hydrogen diffusion under the hydrostatic stress,  $\sigma_h = (\sigma_{xx} + \sigma_{yy} + \sigma_{zz})/3$ , with diffusion constant,  $D_H$ . The hydrogen concentration, temperature, the gas constant, and the molar volume are  $C$ ,  $T$ ,  $R=8.314$  J/mol/K, and  $V_H$ , respectively. The effect of stress is incorporated as the force term acting hydrogen into the equation by considering the change of the volume of hydrogen diffusion sites which is caused by the hydrostatic stress. The Adams-Bashforth method is utilized as the time integration. Both codes are parallelized by the parallel processing computer library MPI.

### 2. Notched Round-Bar Specimen Model

We modeled a half of the notched round-bar specimen, which is used in the tensile test of the paper<sup>6)</sup> and is shown in **Fig. 2**, due to its symmetry. The stress concentration factor

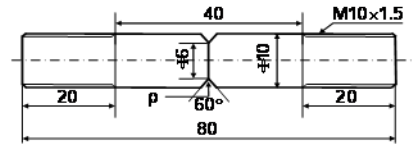


**Fig. 2** Dimension of the notched round-bar specimen<sup>6)</sup>

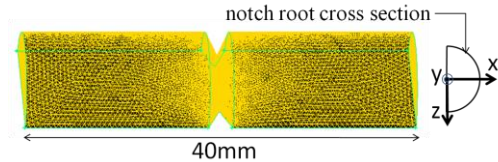


**Fig. 3** Calculation mesh of the notched round-bar specimen and the definition of the coordinate system

of this specimen is  $K_t=4.9$ . The 3-dimensional calculation mesh of the model, which was generated by the code GAMBIT 2.4.6 of Fluent Inc., is shown in **Fig. 3**. In this figure, the notch root cross section means the xz cross section with the minimum area. The mesh consisted of linear tetrahedral elements. The numbers of element and of node are 502823 and 93641, respectively. Since we were interested in the region around the cross section of the notch root, we modeled the part of the notched round-bar specimen in **Fig. 2** within a distance of less than 20 mm from the notch root section.

We used the experimental condition which is reported in the paper<sup>6)</sup> as the condition for calculating the stress and the hydrogen concentration in the notched round-bar specimen model. In the paper,<sup>6)</sup> after charging hydrogen into the notched round-bar specimen in **Fig. 2**, the slow strain rate test (SSRT) is carried out, and the relation between the diffusible hydrogen content and the maximum tensile stress shown in **Fig. 4** is obtained. In this figure, the data which we used as the calculation condition is indicated by Case A and Case B. The diffusible hydrogen means hydrogen which is not trapped strongly by defects at experimental temperature, and is measured by the TDS analysis. The maximum tensile stress is the fracture strength and is given by the maximum tensile load divided by the minimum area of the initial cross section around notch; that is nominal stress. According to the paper,<sup>6)</sup> furthermore, in the range in which the hydrogen content is more than 0.5 mass ppm in **Fig. 4**, the intergranular fracture is observed in the SEM fractography. On the basis of the experimental result in the paper,<sup>6)</sup> we calculated the stress and the hydrogen concentration of two cases which are labeled Case A and Case B in **Fig. 4**. The hydrogen content and the maximum tensile stress of each case are 0.5 mass ppm and 1650 MPa for Case A and 1.95 mass ppm and 650 MPa for Case B, respectively.

In the stress calculation by the elastoplastic analysis of the improved Adventure\_Solid code, we used the following material properties:<sup>13)</sup> the Young modulus,  $E=190.3$  GPa, the yield stress,  $\sigma_Y=1010$  MPa, the Poisson ratio,  $\nu=0.3$ , and the hardening law,  $\sigma[\text{MPa}] = 1251.7\varepsilon^{0.041} + 0.23471$ . We applied the tensile stress of 594 MPa for Case A and of 234 MPa for

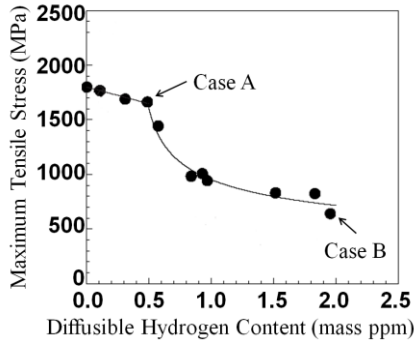


**Fig. 4** Relation between the diffusible hydrogen content and the maximum tensile stress<sup>6)</sup>

Case B on the top and the bottom surfaces of the notched round-bar specimen model in order to estimate the stress of grain boundaries at the moment when the fracture is observed. The value of the applied tensile stress was calculated from the maximum tensile stress in Fig. 4.

For the hydrogen diffusion calculation on the basis of Eq. (1), we used the following parameters<sup>12)</sup>:  $D_H = 4.0 \times 10^{-11} \text{ m}^2/\text{s}$ ,  $V_H = 2.1 \times 10^{-6} \text{ m}^3/\text{mol}$ ,  $T = 293 \text{ K}$ . The hydrostatic stress  $\sigma_h$  was obtained from the result of the stress calculation. As the initial hydrogen concentration in the whole calculation region, we set 1.0 which is the value normalized by the initial hydrogen concentration,  $C_0$ , which was extracted from Fig. 4, at all the nodes because the hydrogen distribution in the specimen is homogenized by keeping at ambient temperature sufficiently before SSRT in the experiment.<sup>6)</sup> As the boundary condition, we gave the Neumann condition with zero flux to all boundaries of the calculation region because the specimen is coated with cadmium to prevent hydrogen desorption after hydrogen is charged.<sup>6)</sup> The calculation was carried out until the hydrogen concentration became steady.

### 3. Polycrystalline Model

The polycrystalline model was a box region of the dimension size  $0.06 \text{ mm} \times 0.12 \text{ mm} \times 0.06 \text{ mm}$  which was divided using the random Voronoi tessellation as done in the paper.<sup>10)</sup> The grain and the grain boundary of polycrystalline materials were modeled by the Voronoi cell and the interface between the Voronoi cells, respectively. Each grain had the different crystallographic orientation as its characteristic. Such a modeling of polycrystalline materials is used in the paper<sup>14)</sup> to evaluate stress at grain boundaries of a nickel polycrystal. In this paper, we considered the polycrystalline model as an inside part of the notched round-bar specimen.

In the calculation of the stress at the grain boundary, we assumed that the polycrystalline model was an elastic material as reported in the paper.<sup>14)</sup> Since in this assumption the stress concentration at the grain boundary easily occurs by small strain, this can be considered as the most severe situation in the intergranular fracture. As the parameters for the elastic analysis, we gave to each grain the following material properties of iron:<sup>15)</sup> the Young modulus  $E_{\text{poly}} = 131.8 \text{ GPa}$ , the Poisson ratio  $\nu_{\text{poly}} = 0.373$ , the shear

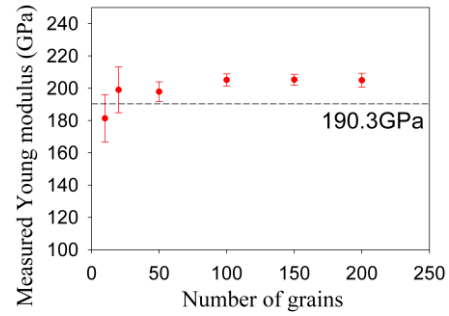


**Fig. 5** The dependence of the measured Young modulus on the number of grains in the polycrystalline model

modulus  $G_{\text{poly}} = 116.0 \text{ GPa}$ . The crystallographic orientation of each grain was specified by the Euler angle generated randomly. As the boundary condition, in order to obtain the stress at the grain boundaries under the tensile test condition, we gave the displacement distribution which was extracted from the calculation result of the notched round-bar specimen model described in the previous section.

Since the crystallographic orientation was given to each grain randomly, it was considered that the number of grains influences the evaluation of stress at grain boundaries. Therefore, we determined the number of grains by measuring the Young modulus of the whole polycrystalline model and by observing its fluctuation. The Young modulus was measured by numerically carrying out the tensile test of the polycrystalline model. In this numerical test, we increased the applied uniaxial tensile load in the  $y$  direction gradually and measured the stress and the strain of the upper cross section of the model. The Young modulus was obtained as the gradient of the measured relation between the stress and the strain. This test was carried out by increasing the number of grains of the polycrystalline model. Furthermore, in order to observe the statistical fluctuation of the Young modulus in each case of the number of grains, we measured the Young modulus of five polycrystalline models which have the different configuration of the grain orientation. The result is shown in Fig. 5. In the figure, the fluctuation of the measured Young modulus is represented by the vertical error bar of the standard deviation. According to the figure, it is found that when the number of grains is larger than 100, the measured Young modulus is almost constant though it is slightly different from the Young modulus of the notched round-bar specimen. The fluctuation becomes small and also almost constant. Hence we used the polycrystalline model with 100 grains. The mesh of the polycrystalline model consisting of 100 grains is shown in Fig. 6. The mesh was generated by the code GAMBIT 2.4.6 of Fluent Inc. and consisted of linear tetrahedral elements as well as the mesh of the notched round-bar specimen model. The numbers of element and of node are 1,051,429 and 187,534, respectively.

We also used the mesh in Fig. 6 for the hydrogen diffusion calculation in the polycrystalline model. The calculation parameter was same as that described in the previous section. We set the hydrostatic stress which was obtained from the stress distribution calculated in the polycrystalline model.

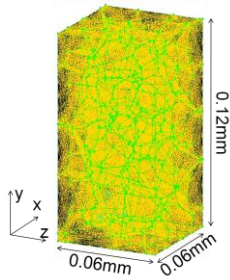


Fig. 6 Mesh of the polycrystalline model

We also set the normalized value 1.0 as the initial concentration condition at all the nodes except the boundary nodes, and used the hydrogen concentration distribution extracted from the calculation result in the notched round-bar specimen model as the boundary condition. The calculation was carried out until the hydrogen concentration became steady.

### III. Calculation Results

#### 1. Notched Round-Bar Specimen Model

Figure 7 shows the hydrostatic stress distribution and the maximum principal stress distribution in the radial direction as a function of the distance from the notch root. The distribution was obtained by averaging in the angular direction on the notch root cross section. In the figure, the stress peak is observed near the notch root. This is the stress concentration caused by the plastic constraint due to the multiaxial stress condition around the notch root. The peak position depends on the stress concentration factor calculated from the shape of the notch root, and also depends on the applied load. Figure 8 shows the hydrogen concentration distribution in the radial direction as well as Fig. 7. The figure shows the distribution obtained after the hydrogen concentration became almost steady, that is after 1,000 min diffusion. It is observed in the figure that hydrogen gathers around the stress peak in Fig. 7. The same tendency as both figures is also seen in the 2-dimensional calculation of the paper.<sup>12)</sup> Since it is reported that the hydrogen embrittlement of steels is controlled by the maximum principal stress and the hydrogen concentration at the peak location,<sup>16)</sup> in the next section, we evaluated the stress and the hydrogen concentration of grain boundaries at the peak position using the polycrystalline model.

#### 2. Polycrystalline Model

In the calculations of stress and hydrogen concentration in the polycrystalline model, we used data extracted from the calculation results of the notched round-bar specimen model as the boundary condition. For the stress calculation, the displacement distribution on the surface of a box region which was placed inside the notched round-bar specimen model was given to the surface of the polycrystalline model as the boundary condition. The box region had the same dimension as the polycrystalline model, and was placed at the stress concentration part on the notch root cross section. To be exact, using the coordinate system of the notched round-bar specimen model, the position of the center of the

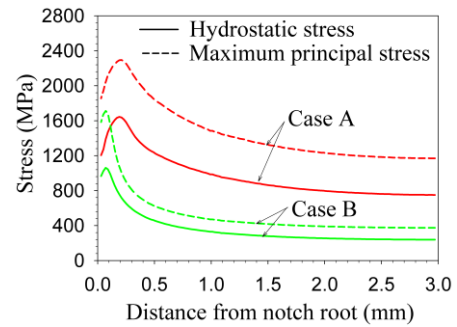


Fig. 7 Calculated distributions of hydrostatic stress and of maximum principal stress on the notch root cross section

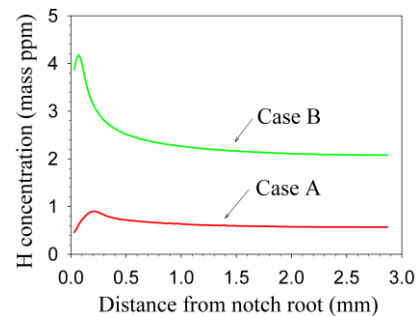
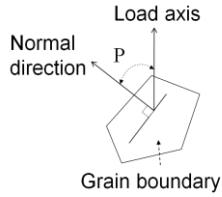


Fig. 8 Calculated hydrogen concentration distribution on the notch root cross section

inside box region was (2.81 mm, 0.0 mm, 0.0 mm) for Case A, and (2.93 mm, 0.0 mm, 0.0 mm) for Case B. These positions were determined from the result in Fig. 7. Note the origin of the x coordinate is at the center of the notch root cross section as shown in Fig. 3. For the hydrogen diffusion calculation, the hydrogen concentration distribution on the surface of the box region was given to the surface of the polycrystalline model as well as the boundary condition of the stress calculation. The hydrostatic stress distribution obtained by the stress calculation in the polycrystalline model was also used for the hydrogen diffusion calculation. The calculation was carried out until the hydrogen concentration became steady.

By defining the orientation of the grain boundary as the inclination of the grain boundary against the load axis as shown in Fig. 9, we obtained the relation between the averaging normal stress of the grain boundary and the orientation of the grain boundary from the result of the stress calculation as shown in Fig. 10. In Fig. 10(a), the error bar means the fluctuation due to the different crystallographic orientation.

The normal grain boundary stress was averaged in the results obtained from five statistically different configurations of the grain orientation. In Fig. 10, the result of the case that the crystallographic orientation is isotropic is also shown for comparison. Figure 11 shows the relation between the hydrogen concentration and the grain boundary orientation. This figure shows for the one case of the crystallographic orientation.



**Fig. 9** Definition of the grain boundary orientation

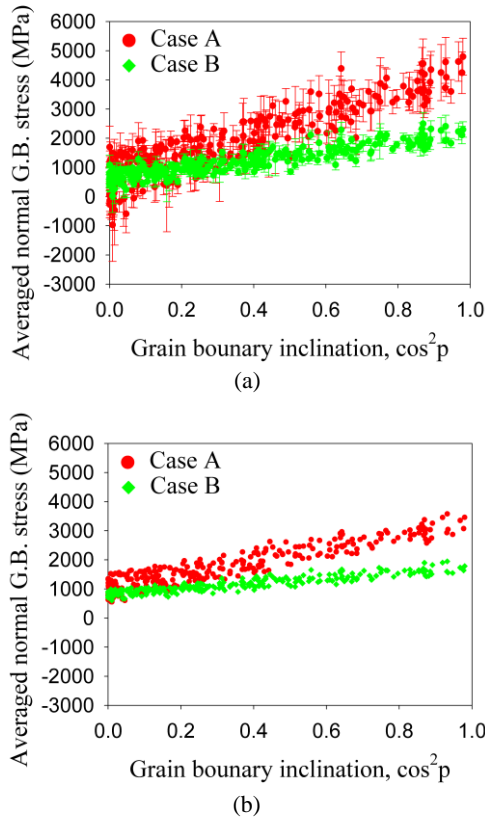


**Fig. 10** Relation between the normal grain boundary stress and the grain boundary orientation: (a)The case of anisotropic crystallographic orientation, (b)The case of isotropic crystallographic orientation.

#### IV. Discussion

According to Fig. 10, it is seen that the averaged normal grain boundary stress of the anisotropic case (a) scatters in the broader range than the isotropic case (b). Thus, it is seen that the crystallographic anisotropy influences the grain boundary stress remarkably. Since the normal grain boundary stress increases in proportion to  $\cos^2 p$  if a uniaxial load is applied to an isotropic polycrystalline model, the broadly scattering of the normal grain boundary stress in Fig. 10(b) indicates the effect of the multiaxial stress condition of the stress concentration part of the notched round-bar specimen. Therefore it is considered that the calculation result in Fig. 10(a) shows the proper tendency of the grain boundary stress in the notched round-bar specimen strained in SSRT. In Fig. 11, it is not observed that hydrogen gathers around the grain boundary which has the large normal stress as the

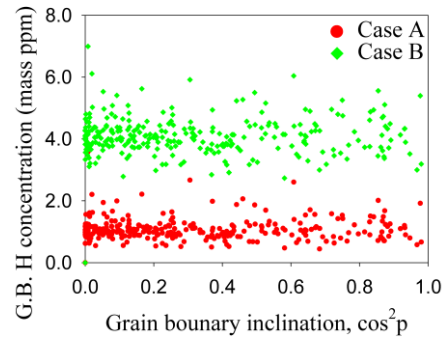


**Fig. 11** Relation between the hydrogen concentration and the grain boundary orientation

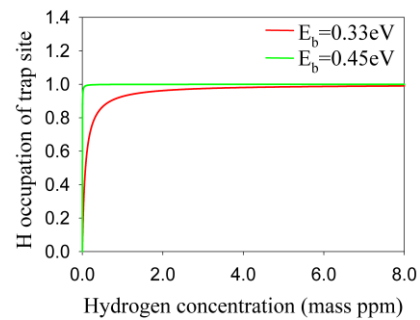


**Fig. 12** Relation between the hydrogen occupation ratio of the grain boundary trap site and the hydrogen concentration

case of hydrogen in the notched round-bar specimen model. As seen in Eq. (1), this is because the driving force of hydrogen migration is in proportion to the gradient of hydrostatic stress. It is also found that the maximum hydrogen concentration at the grain boundary becomes at most four times larger than the peak value in the notched round-bar specimen model.

Next we consider the crack initiation in the grain boundary hydrogen embrittlement. In the decohesion model, since hydrogen which is trapped by grain boundaries weakens their strength, the fracture strength of steels decreases. The strength of the grain boundary depends on the hydrogen occupation ratio of the trap site of the grain boundary. The hydrogen occupation ratio is determined by the hydrogen concentration around the trap site and the binding energy between the trap site and hydrogen. In the papers,<sup>17,18)</sup> the fracture strength and the binding energy for the bcc Fe S3(111) symmetrical tilt grain boundary, which is simple but has high grain boundary energy, 1.52 J/m<sup>2</sup>, are evaluated using the first-principles calculation code, the Vienna Ab initio Simulation Package (VASP)<sup>19)</sup>. The grain boundary is modeled using 36 iron atoms and its tilt angle is 70.5 deg. According to the papers, the binding energy depends on the number of the hydrogen atoms trapped by the grain boundary, and the maximum and the average value are 0.45 eV and 0.33 eV, respectively. When no hydrogen atoms are trapped at the grain boundary, the fracture strength is about 22 GPa, and it becomes about 13 GPa in the case that the grain boundary is fully occupied by hydrogen atoms.

Using the binding energy evaluated by the first-principles calculation, we obtained the relation between the occupation ratio and the hydrogen concentration from the consideration of the local equilibrium<sup>20)</sup> as shown in Fig. 12.

From Fig. 11 and Fig. 12, it is found that the more than 80% trap sites of the most grain boundary were occupied by hydrogen. Furthermore, according to the first-principles calculations, the fracture stress decreases to about 13 GPa in the case that the trap sites of the grain boundary are filled with hydrogen. In Fig. 10(a), however, the maximum of the normal grain boundary stress is about 6 GPa for Case A and about 2 GPa for Case B. The evaluation in the atomic level was at least 2.2 times larger than the calculation in this paper. Therefore, even though the elastic analysis was applied to the stress calculation, the grain boundary stress did not reach the fracture stress evaluated in the atomic level. According to this result, it is considered that the crack at the grain boundary cannot be initiated only by the stress concentration due to the crystallographic anisotropy. Hence we can think that the stress concentration for the crack initiation at the grain boundary needs other factors such as the dislocation accumulation at inclusions like carbides.

## V. Summary

We calculated the stress and the hydrogen concentration using the notched round-bar specimen model under the tensile test condition. Furthermore, using the calculation results of the notched round-bar specimen model, we evaluated the stress and the hydrogen concentration at the grain boundary using the polycrystalline model which has the crystallographic anisotropy. As a result, the crystallographic anisotropy and the multiaxial condition at the stress concentration part of the notched round-bar specimen influenced remarkably the normal grain boundary stress. It was found that the stress concentration which can initiate the intergranular fracture does not occur by the crystallographic anisotropy.

## Acknowledgment

This study was carried out as a part of research activities of "Fundamental Studies on Technologies for Steel Materials with Enhanced Strength and Functions" by Consortium of JRCM (The Japan Research and Development Center of Metals). Financial support from NEDO (New Energy and Industrial Technology Development Organization) is gratefully acknowledged.

## References

- 1) J. Lufrano, P. Sofronis, H. K. Birnbaum, "Elastoplastically accommodated hydride formation and embrittlement," *J. Mech. Phys. Solids*, **46**, 1497-1520 (1998).
- 2) H. K. Birnbaum, P. Sofronis, "Hydrogen-enhanced localized plasticity---a mechanism for hydrogen-related fracture," *Mater. Sci. Eng.*, **A176**, 191-202 (1994).
- 3) C. J. McMahon, Jr., "Hydrogen-induced intergranular fracture of steels," *Eng. Fract. Mech.*, **68**, 773-788 (2001).
- 4) S. Serebrinsky, E. A. Carter, M. Ortiz, "A quantum-mechanically informed continuum model of hydrogen embrittlement," *J. Mech. Phys. Solids*, **52**, 2403-2430 (2004).
- 5) M. Nagumo, "Hydrogen related failure of steels - a new aspect," *Mater. Sci. Technol.*, **20**, 940-950 (2004).
- 6) M. Wang, E. Akiyama, K. Tsuzaki, "Hydrogen degradation of a boron-bearing steel with 1050 and 1300 MPa strength levels," *Scripta Mater.*, **52**, 403-408 (2005).
- 7) M. Yamaguchi, K. Ebihara, M. Itakura, T. Suzudo, H. Kaburaki, "First-principles study on the hydrogen embrittlement of grain boundaries of iron," *Proceedings of Symposium at 160th ISIJ meeting*, 59-66 (2010).
- 8) Y. Sato, K. Fujita, H. Suzuki, K. Takai, Y. Hagihara, N. Ishikawa, "Hydrogen desorption spectra from various trapping sites using thermal desorption spectrometry detected from low-temperature," *CAMP-ISIJ*, **22**, 559 (2009).
- 9) K. Ebihara, H. Kaburaki, T. Suzudo, K. Takai, "A Numerical Study on the Validity of the Local Equilibrium Hypothesis in Modeling Hydrogen Thermal Desorption Spectra," *ISIJ Int.*, **49**, 1907-1913 (2009).
- 10) M. Itakura, H. Kaburaki, C. Arakawa, "Branching mechanism of intergranular crack propagation in three dimensions," *Phys. Rev.* **E71**, 055102-1-4 (2005).
- 11) ADVENTURE Project, <http://adventure.sys.t.u-tokyo.ac.jp>, (2010).
- 12) M. Wang, E. Akiyama, K. Tsuzaki, "Determination of the critical hydrogen concentration for delayed fracture of high strength steel by constant load test and numerical calculation," *Corr. Sci.*, **48**, 2189-2202 (2006).
- 13) E. Akiyama, private communication.
- 14) M. Kamaya, Y. Kawamura, T. Kitamura, "Three-dimensional local stress analysis on grain boundaries in polycrystalline material," *Int. J. Solids Struct.*, **44**, 3267-3277 (2007).
- 15) S. Nagasima, *Syugou Soshiki*, Maruzen, Tokyo, 262 (1984).
- 16) M. Wang, E. Akiyama, K. Tsuzaki, "Effect of hydrogen and stress concentration on the notch tensile strength of AISI 4135 steel," *Mater. Sci. Eng.*, **A398**, 37-46 (2005).
- 17) M. Yamaguchi, "First-Principles Study on the Grain Boundary Embrittlement of Metals by Solute Segregation: Part I. Iron (Fe)-Solute (B, C, P, and S) Systems," *Metall Mater Trans. A*, **42**, 319-329 (2011).
- 18) M. Yamaguchi, K. Ebihara, M. Itakura, T. Kadoyoshi, T. Suzudo, H. Kaburaki, "First-Principles Study on the Grain Boundary Embrittlement of Metals by Solute Segregation: Part II. Metal (Fe, Al, Cu)-Hydrogen (H) Systems," *Metall. Mater. Trans.*, **A42**, 330-339 (2011).
- 19) G. Kresse, J. Hafner, *Phys. Rev.*, **B47**, 558-61 (1993); G. Kresse, J. Furthmüller, *Phys. Rev.*, **B54**, 11169-11186 (1996); G. Kresse, D. Joubert, *Phys. Rev.*, **B59**, 1758-1775 (1999).
- 20) Oriani, "The diffusion and trapping of hydrogen in steel," *Acta Metall.*, **18**, 147-157 (1970).